Condensed DNA in Lipid Microcompartments

Shahriar Osfouri,[†] Pasquale Stano,[‡] and Pier Luigi Luisi*

Institut für Polymere, ETH Zentrum, Universitätstrasse, 6, CH-8092 Zurich, Switzerland

Received: June 8, 2005; In Final Form: August 1, 2005

DNA was studied in lipid reverse micelles with the aim of investigating the interactions of DNA with lipids in a restricted compartment with minimal water content. Circular dichroic (CD) spectra of DNA at low water content showed the characteristic polymer-salt-induced (psi) spectra of condensed DNA. Dynamic light scattering showed a peak around a radius of 400 nm (corresponding to DNA-containing micelles), and a peak around 2.5 nm (corresponding to "empty" micelles). Fourier Transform-IR (FT-IR) spectroscopy was carried out and analyzed in terms of three distinct states of water inside the micelle water pool, where the local concentration of DNA reached an estimated value of ca. 600 mg/mL, comparable to that found in restricted biological compartments.

Introduction

In biological structures, very long strings of nucleic acids are often segregated into very small compartments having a radius exceedingly smaller than the stretched length of the guest macromolecules. For example, the entire genome of a eukaryotic cell is localized in its nucleus.[1] DNA concentrations have been estimated to be ca. 20, 100, or 800 mg/mL in a bacteria nucleoid, in a small-nucleus eukaryotic cell, and in the bacteriophage's head, respectively.[2] The biophysics of the process of folding and compaction is still intriguing,[3] especially in view of the fact that DNA is highly charged. Likewise, although the physiological significance of DNA ternary and quaternary modifications seems to be straightforward,[4] the factors and mechanisms that control and modulate the process are not well understood.

The term condensed is often used to indicate the particular structure assumed by DNA under those tightly packed conditions. Models of the compaction of DNA in vitro have been presented.[5] It has been shown, for example, that DNA can assume a condensed form under the action of certain polymers in the presence of a high salt concentration,[6,7] multivalent ions,[8−10] cationic liposomes,[11,12] basic proteins,[13,14] and alcohols.[15−17] Structures and phase transitions of DNA condensed phases have been reviewed by Livolant and Leforestier.[18] Usually, as a criterion for the condensed form, the anomalous CD spectrum is presented,[19] for which the term "psi spectrum" has been coined (for polymer-salt-induced spectrum), sometimes abbreviated as ψ-spectrum. This is characterized by a considerable enhancement of ellipticity in the 260−280 nm region, and by a broad band at longer wavelengths (300−350 nm), at which the not-condensed DNA in aqueous solution shows no signal. This anomalous long wavelength signal is probably due to scattering arising from the three-dimensional network of condensed DNA.[20] The magnitude of the 260−280 nm CD signal reflects the extent of compactness and the long-range order of the condensed particles,[4,9] which have sometimes been visualized as toroidal or bent stem structures by electron microscopy analysis.[4] These extended and supramolecular chiral arrays, which are liquid crystalline states of DNA, are responsible of the ψ-type CD spectrum.

More recently, on the basis of an earlier, preliminary report,[21] we could show that DNA can assume a condensed form, with the typical ψ-spectrum, when solubilized in reverse micelles.[22] Reverse micelles are formed when certain surfactants are dissolved in apolar solvents (more typically alkanes) in the presence of a minute amount of water (typically 0.5−2% v/v). Water is concentrated in the so-called water pool, and the lipid (or other surfactant molecules) constitutes the interface between the organic and the aqueous phase. It was shown several years ago that enzymes, and even microorganisms, can be solubilized in the water pool without a loss of activity, giving rise to enzymology and microbiology in essentially apolar solvents.[23] The radius of the reverse micelles is typically around 0.5−5 nm, depending on the water content, and of course the introduction of a large macromolecular component brings about rearrangements of the size and structure of reverse micelles. Previous works on DNA or polynucleotides in reverse micelles have been carried out with charged surfactants, namely CTAB (hexadecyltrimethylammonium bromide),[21,24,25] or AOT (bis-(2-ethylhexyl)sodium sulfosuccinate).[22] Very recently, the entrapment and condensation of DNA in neutral reverse micelles (composed by the nonionic surfactant tetraethyleneglycol dodecyl ether) has been reported.[26]

The surfactants used until now for DNA-containing reverse micelles are, however, not very attractive from the biological point of view. It would be more interesting to use lipids so that the incorporation of DNA into reverse micelles would also reflect the interaction between lipid and DNA. It is known, in fact, that the eukaryotic cell nuclear envelope is constituted in large part by lipids;[27,28] furthermore, in recent years, the interaction between lipid and nucleic acids has been the subject of intense investigation.[29−31] In this work, we will make use of lecithin reverse micelles, which were shown some time ago to host enzymes without a loss of activity.[32]

* Corresponding author. Present address: Dipartimento di Biologia, Università degli Studi di Roma Tre, Viale Marconi, 446, 00146 Roma, Italy. Tel.: +39.06.55176329. Fax: +39.06.55176321. E-mail: luisi@mat.ethz.ch.

[†] Present address: Department of Chemical Engineering, Persian Gulf University, Boushehr, Iran. Tel.: +98 771 4222174. E-mail: osfouri@pgu.ac.ir.

[‡] Present address: Dipartimento di Biologia, Università degli Studi di Roma Tre, Viale Marconi, 446; 00146 Roma, Italy. E-mail: stano@uniroma3.it.

10.1021/jp053057m CCC: $30.25
Published on Web 10/04/2005

Another important question connected with DNA condensation is the hydration state of the DNA molecules. In fact, there is some evidence that all the relevant factors that affect the DNA packaging have a relation with the reorganization and the state of the water along the DNA chains.[4,9,24,26] The structure of water is an important element of the molecular interactions in reverse micelles; several studies have been devoted to this question in the past few years.[33−36]

In a small compartment, as in the case of a DNA-containing reverse micelle, there is a limited number of water molecules, and the question is whether this can be considered as free water or instead is all "frozen" and competitively distributed between the polynucleotides and the lipid cell walls.

In this work, we will use infrared spectroscopy in order to investigate the water state in lecithin reverse micelles, with or without DNA. In addition to circular dichroism, a detailed analysis of the size distribution of reverse micelles will be carried out by dynamic light scattering measurements. Combining these three techniques, we propose a simple model for DNA compaction in reverse micelles.

Experimental Section

Materials. 1,2-Dioctanoyl-*sn*-glycero-3-phosphocholine (C_8PC) was purchased from Avanti Polar Lipid Inc. (Alabaster, AL). Herring testes DNA (41.2% G-C content), isooctane, and 1-hexanol were purchased from Fluka (Buchs, Switzerland). All aqueous solutions were prepared by dissolving DNA in 10 mM Tris-HCl and 1 mM EDTA buffer at pH 7. DNA ladder samples (100−1000 and 500−10000 bp) were from Sigma (codes P1473 and D0428, respectively).

DNA Sonication and Characterization. Herring testes DNA was sonicated for a total of 28 min (4 × 7 min, output power 35 W, duty cycle 50%) in ice and under nitrogen, using a tip sonicator (model W-225R, Heat System Ultrasonics Inc., Plainview, NY) according to standard DNA sonication procedures that reduce to a minimum the risk of DNA degradation. The resulting fragments comigrate in gel electrophoresis (2% acrylamide) with marker DNA in the 100−800 bp range. DNA was further characterized by zeta-potential measurements, by means of electrophoretic light scattering experiments carried out at 25 °C on a Zetasizer 5000 instrument (Malvern Instruments) equipped with a ZET5104 electrophoretic cell. DNA was dissolved in water, 10 mM Tris HCl, and 1 mM EDTA buffer (pH 7.0) to concentrations of 4, 1, and 0.5 mg/mL, and then the zeta-potential was calculated by averaging 10 different consecutive measurements. Data were analyzed using the instrument's built-in fitting algorithm (Malvern Software, PCS version 1.61) with the following parameters: order of fit = 5; F(ka) = autoselected; range = ±200 mV.

Reverse Micelle Preparation and Characterization. In reverse micellar solution, the concentration of C_8PC and the volume percentage of 1-hexanol were 50 mM and 10%, respectively, in all samples. To remove dust, we filtered the solution of C_8PC/isooctane/1-hexanol with Millex-GV 0.22 μm filters (Millipore, Bedford, MA). Using a direct-injection method, we solubilized DNA with different initial concentrations in the isooctane/1-hexanol reverse micellar solution, and mixed the solution with a vortex stirrer for 1 min. Reverse micelle solutions are characterized by the value w_0, which simply represents the ratio between the molar concentration of water and the surfactant.

The UV−vis absorption spectra were recorded at 25 °C on a Cary 1E Varian spectrophotometer, using quartz cells with path lengths 1 and 2 cm. The CD measurements were carried out at 25.0 °C using the JASCO J-600 spectropolarimeter with a quartz cell having a 0.5 cm path length. For each sample, nine acquisitions were averaged. Instrumental ellipticitiy was converted into molar ellipticity (θ), considering 1 dmol of base pairs to be equivalent to 65 g of DNA.

The size distributions of reverse micelles were obtained by dynamic light scattering. The measurements were performed on a home-assembled light-scattering photometer, made of a 25 mW He−Ne laser (model 127, Spectra-Physics Lasers, Mountain View, CA), a DLS/SLS-5000 compact goniometer system (ALV, Langen, Germany), two SPCM-AQR avalanche photodiodes (PerkinElmer Optoelectronics, Vaudreuil, Canada), and a 5000 multiple-tau digital correlator (ALV). The scattering cells were immersed in a fuzzy-thermostatic decalin bath at 25.0 °C. For each sample, the measurements were repeated 10 times at various angles. Details for the DLS-based data manipulation needed to estimate the DNA concentration in reverse micelles are reported in the Supporting Information.

FT-IR absorption spectra for all samples were recorded in the range of 400−4000 cm^{-1} with a VECTOR 22 Bruker spectrophotometer (Karlsruhe, Germany) using a CaF_2 window cell (0.05 mm path length) at room temperature (25 °C). To obtain good quality spectra, each sample was recorded with 32 scans at an effective resolution of 2 cm^{-1}. Deconvolution of the hydroxy stretching vibration band (3000−3700 cm^{-1}) was performed using the built-in Levenberg−Marquardt algorithm of the OPUS 3.0 software package (Bruker). Typical values of the fitting reduced chi squared (χ_{red}^2) were of ca. 10^{-5} (three components). The relative amount of a certain OH stretching mode has been calculated by dividing the area of the corresponding Gaussian component by the total integrated area of the band.

$$P_j = \frac{A_j}{A_{tot}}$$

$$\sum_j P_j = 1$$

Using the P_j values, it is a common procedure to calculate the number of water molecules associated to a certain type of OH stretching mode, as $n_j = w_0 \times P_j$.

Results

Short chain lecithin (dioctanoyl phosphatidylcholine, C_8PC) reverse micelles, produced by injecting a water solution (with or without DNA) into a preformed lecithin organic solution, have been analyzed and characterized by UV−vis, CD, dynamic light scattering, and FT-IR techniques. In the following discussion, DNA concentration refers to the aqueous stock solution. The water content of the reverse micelle phase, as commonly used in the literature, is given as w_0, the molar ratio between water and surfactant.

Herring testes DNA (41.2% G-C content; T_m = 87.5 °C in 0.15 M NaCl, 15 mM sodium citrate) is available as a very high molecular weight compound. Its size can be decreased by sonication (Figure 1) to obtain a less viscous aqueous solution. In addition, the mean size and the size distribution of the DNA obtained by this protocol have been determined by image analysis. Our data indicate an average size of 285 bp with a half-height width of 325 bp (see Supporting Information). Sonicated DNA in 10 mM Tris HCl, 1 mM EDTA buffer (pH

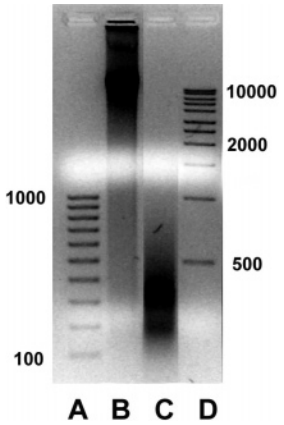

Figure 1. Gel electrophoresis of herring testes DNA (molecular weight increases going from the bottom to the top). (A) Low molecular weight DNA ladder (100−1000 bp). (B) Herring testes DNA before sonication. (C) Herring testes DNA after four cycles of sonication (7 min each, total sonication time 28 min). (D) High molecular weight DNA ladder (500−10000 bp).

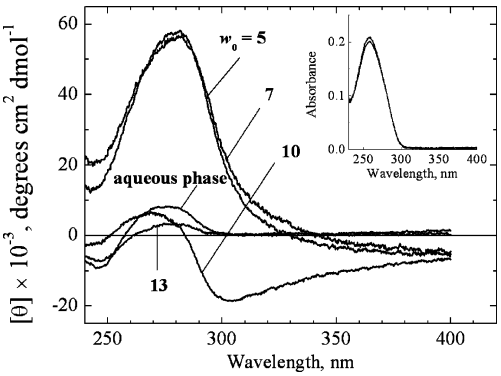

Figure 2. CD spectra of DNA in C_8PC reverse micellar solution with different w_0 values and an initial concentration of 2 mg/mL DNA in aqueous stock solution. $w_0 = 5$, 7, 10, and 13. The CD spectrum of an aqueous DNA solution with the same concentration as in the case $w_0 = 13$ is shown for comparison purposes. In the inset, UV−vis spectra of DNA in reverse micelle ($w_0 = 7$) and water are shown.

7.0) has been further characterized by zeta-potential, as obtained by electrophoretic light scattering measurements. The concentration-independent value of −36 mV was obtained in the DNA concentration range of 0.5−1.5 mg/mL. Higher DNA concentrations (e.g., 2 and 4 mg/mL) gave lower zeta-potential values (−49 and −53 mV, respectively).

In the following discussion, the interest will focus on DNA condensation in lecithin reverse micelles under the experimental conditions selected for this work, with particular attention to the w_0 and DNA concentration effects. Other factors, such as the DNA size, the DNA base composition, and the counterion effect, will not be investigated.

Circular Dichroism. We first carried out a CD analysis as a function of w_0 with a constant DNA (2 mg/mL in the aqueous phase) and lecithin concentration of 50 mM. Results are shown in Figure 2.

It is apparent that there is a large enhancement of the dichroic signal at lower values of w_0, with all distinctive signs of a ψ-spectrum: not only the higher intensity in the 260−280 nm region but also the appearance of a significant band at a wavelength higher than 350 nm. In contrast, at $w_0 = 13$ the difference with DNA dissolved in water is not significant. The spectrum at $w_0 = 10$ is somewhat anomalous; we will come back to this point later on. The same features as in Figure 2 are

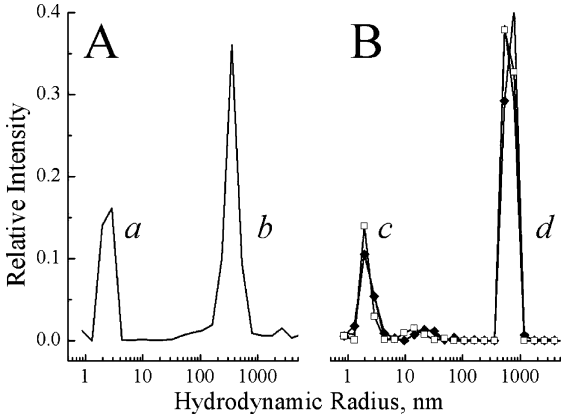

Figure 3. DLS size distribution (ILT, 120°) of a C_8PC reverse micellar solution containing aqueous DNA solution, $w_0 = 5$: (A) 0.5 mg/mL of DNA and (B) 4 mg/mL of DNA. In panel B, three size distributions are plotted, referring to 15 min (line), 1 day (diamonds), and 6 days (squares) from the preparation of the micellar solution.

observed in the case of a DNA concentration of 1 mg/mL (Figure S3, Supporting Information).

Comparing the case $w_0 = 7$ with that of $w_0 = 10$, it seems as if there is a transition with the onset of a strong negative band in the higher wavelength region before the spectrum levels off, at $w_0 = 13$, at the aqueous value. The CD spectrum at $w_0 = 10$ is composed of a negative differential scattering band at a wavelength higher than 300 nm, and of a strong positive contribution in the 260−280 nm range, loosely resembling the shape of a Z-DNA form.[37] Interestingly, no size transitions of the micellar structure has been detected from $w_0 = 10$ to $w_0 = 13$ (DLS data, not shown). From these observations, we conclude that a fine-tuning of the hydration forces can lead to relevant DNA structural transition. Lipid and DNA compete for water molecules in the micellar system, in which there is a limited amount of water.

It should also be noticed that the spectra of Figure 2 (as well as the samples prepared using 1 mg/mL DNA) are constant with time, as shown by repeated measurements up to 24 h.

UV absorption spectra were also recorded. As shown in the inset of Figure 2, reverse micelle samples had the same UV−vis spectrum of a corresponding sample in which the organic phase is not present, that is, an aqueous DNA solution of the same concentration.

Dynamic Light Scattering (DLS). Figure 3A shows the size distribution, as determined by DLS, of a micellar solution with $w_0 = 5$ and containing DNA at a concentration of 0.5 mg/mL in the aqueous phase. DLS analysis at different angles gave the same results, indicating the presence of two well-defined populations. The value of 120° in Figure 3 has been chosen in order to better evidence the smaller component.

The peak centered at around 2−3 nm represents the empty reverse micelles: in fact, a single peak centered at 2−3 nm is also observed when a reverse micellar solution at $w_0 = 5$ is analyzed in the absence of DNA (data not shown). The second peak is centered at around 400 nm, and represents the DNA-containing compartments.

Similar features are detected using a higher DNA concentration (4 mg/mL). In this case (Figure 3B), whereas the empty micelle peak is still centered around 2−3 nm, the filled micelle peak is shifted to ca. 700 nm.

The two-peak system has also been observed in our previous studies with nonlipidic surfactants,[22] but in that case a significant change with time was observed for the larger peak, with the tendency to disappear within 1 day. On the contrary, the two

TABLE 1: Estimation of Condensed DNA Concentration in Reverse Micelles[a] by Means of Mie Analysis of DLS Data

population	mean hydrodynamic radius[b] (nm)	average aggregation number[c]	relative Mie scattering factor[d]	micelle number (mL^{-1})	cumulative internal volume[e]		DNA concentration[f] (mg/mL)
					μL/mL	%	
a	2.5	44	1	1×10^{18}	9.4	99.9	0
b	400	3.1×10^6	1.4×10^8	7×10^7	0.008	0.1	~600
c	2.5	39	1	1.3×10^{18}	7.8	99.6	0
d	700	9.6×10^6	4.6×10^8	2.9×10^7	0.035	0.4	~850

[a] Fifty mM C_8PC reverse micellar solution in isooctane/1-hexanol ($w_0 = 5$) containing DNA. Initial aqueous DNA stock solution concentration was 0.5 mg/mL (entries a and b) or 4 mg/mL (entries c and d). Computed values should be considered with an estimated error of ±20−25%, as calculated by considering the errors associated with all the parameters involved. [b] Monodisperse populations are assumed here for simplicity; cumulative internal volumes and DNA final concentrations are calculated using a size distribution. Although different procedures produce slightly different results, the main conclusions that can be drawn from these calculations are not affected. [c] Number of phospholipid molecules that form a reverse micelle of a given size. The inner surface was calculated by assuming a lipid thickness of 1 nm, and a value of 0.64 nm^2 was used to estimate the headgroup surface (a_0) of a lecithin molecule. [d] Calculated using the Mie theory for homogeneous spherical scatters, using 632.8 nm monochromatic radiation, at a scattering angle of 120° and unpolarized scattered light. Refractive indices used: 1.425 (empty reverse micelles), 1.36 (DNA-filled reverse micelles), 1.3925 (solvent). [e] For 50 mM phospholipid concentration and $w_0 = 5$, the amount of added aqueous solution is 4.5 μL/mL. Discrepancy could derive from the reverse micelle number calculation, which involves many simplified hypotheses and other geometrical simplifications, such as that monolayer thickness and lipid headgroup areas are constant with respect to size and micelle composition. [f] Where 100% DNA trapping is assumed.

lecithin reverse micelle populations show considerable time stability: for up to one week, the shape of the size distribution did not change. In addition, DLS results were rather easily reproduced.

The relative peak intensity in a DLS size distribution, unfortunately, does not represent the relative amount of a particle's population; i.e., the size distribution is intensity-weighted and not number-weighted. In other words, particles are represented in a DLS size spectrum according to their ability to scatter light. It follows that, according to the higher scattering ability of large particles, they are generally over-represented with respect to smaller ones. It would be interesting to calculate, under certain simplifying assumptions (spherical geometry), the relative amount of empty and DNA-filled reverse micelles. Dynamic light scattering analysis, as shown in Figure 3A,B, clearly indicates the presence in the sample of two narrow populations of reverse micelles. We used Mie scattering theory (see Supporting Information) to calculate the scattering efficiencies of small (hydrodynamic radius around 2.5 nm) and large (400 and 700 nm mean radius, see panels A and B of Figure 3, respectively) spherical micelles. Combining these values with the raw DLS data and geometrical considerations, we were able to estimate the relative number of empty and DNA-filled reverse micelles.

For example (see Figure 3B), consider two monodispersed populations of spherical reverse micelles with radii of 2.5 and 700 nm, and suppose the headgroup surface of lecithin molecules is constant ($a_0 \approx 0.64$ nm^2); then, one large micelle corresponds to ca. 80 000 empty reverse micelles. In particular, as the aggregation number is proportional to the surface of a reverse micelle, it follows that $(R_2/R_1)^2$ small reverse micelles (with radius R_1) provide enough surfactant molecules to make a larger reverse micelle (with radius R_2).

The relative ability to scatter light at 120° is on the order of 5×10^8, as calculated by Mie theory. It is clear that DLS analysis allowed for the detection of the small-size population of empty reverse micelles because of that population's overwhelming number of particles. On the other hand, the peak corresponding to DNA-filled reverse micelles actually represents a relatively small fraction of the particle distribution.

Detailed calculations are summarized in Table 1, which shows the elaboration of the data represented in Figure 3A,B (the procedure is described in the Supporting Information).

The systems were modeled as two narrow populations of empty and DNA-filled spherical reverse micelles, differing only in the initial DNA concentration in the aqueous stock solution (0.5 and 4 mg/mL). Furthermore, 100% DNA trapping in the large reverse micelle was assumed. The size of the DNA-filled reverse micelles, being about 400 and700 nm in the two cases (populations b and d in Figure 3, respectively), is a consequence of the different aqueous DNA concentrations of the stock solution used to prepare the micelles. Modeling the system as monodisperse or polydisperse populations does not affect the main conclusion of the analysis. On the basis of the Mie scattering efficiency factors and the DLS results, we estimated the ratio of the two kinds of micelles. The absolute number of particles is then calculated by taking into account the surfactant mass conservation equation and the geometrical packing parameters.

Although the number of small empty reverse micelles is, not surprisingly, orders of magnitude greater than the number of large DNA-filled reverse micelles, the ratio between the cumulative internal volumes (filled:empty) is on the order of 10^{-3} (notice that the ratio between the individual internal volumes for the two kinds of particles is ca. 2×10^7). This extreme disparity in the occupied volumes has an important consequence as far as the concentration of DNA is concerned. In particular, a very significant concentration of nucleic acid is expected in the larger compartments, which is probably related to the DNA structure transition. This means that, considering the DNA entrapped in the internal phase of the larger micelles, a dramatic DNA local concentration of about 700 mg/mL was calculated in both cases (Table 1, last column), leading to the condensed form. These calculations are in agreement with the CD spectra shown above (Figure 2), and give (even if approximately, because of the problems of DLS profile measurements and correct Mie factor estimations) an idea about the concentration of segregated DNA.

FT-IR Water Analysis. The IR spectrum of the reverse micelle solution shows a broad asymmetric band in the region between 3000 and 3700 cm^{-1}, which is similar but not identical to the spectrum of pure water. In particular, several authors have investigated the water OH stretching band by means of deconvolution procedures, to obtain information about the state of water entrapped in the reverse micelles. Several studies have been conducted on the aerosol OT (AOT) surfactant,[33−36,38−40] as well as on lecithin-based systems.[41−44] The deconvolution method consists of the fitting of the observed peak with a number of Gaussian functions, each one representing one characteristic OH stretching frequency of water molecules. The

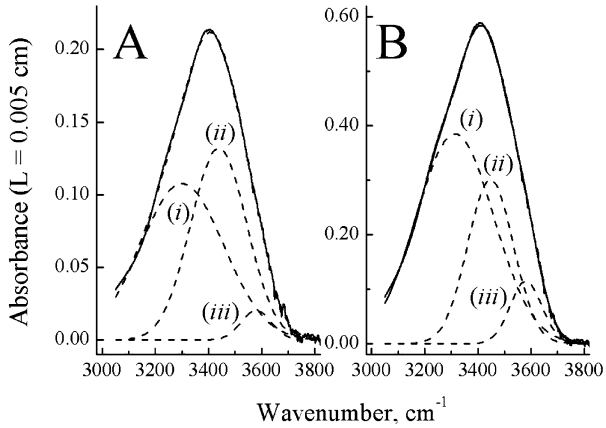

Figure 4. Deconvolution bands of water stretching in C_8PC reverse micellar solution at $w_0 = 10$ (A) and 20 (B). Band (*i*) corresponds to bulklike-type water in the inner core of the micelles, band (*ii*) to the interfacially bound water molecules, and band (*iii*) to trapped water between the lipid hydrophobic chains.

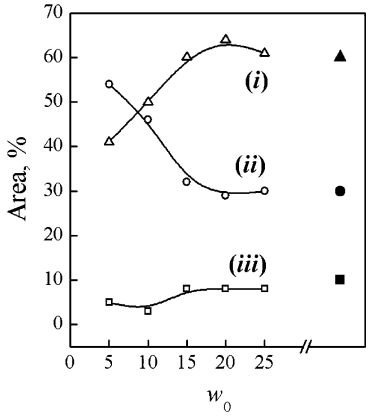

Figure 5. Variation of the peak areas with w_0, obtained by the three-component fittings. Open symbols refer to reverse micelles prepared in the absence of DNA, and filled symbols refer to pure water OH stretching band fitting.[38]

values of the stretching frequencies are generally correlated to a particular state of water molecules, e.g., free water, bound water, bulklike water, etc. As for the number of peaks to be used in the deconvolution procedure, several approaches have been presented in the literature. Two,[44] three,[33,38,39] and four[35,36,40] Gaussian components have been used; in addition, according to other techniques (NMR, electron spin resonance, differential scanning calorimetry), several types of water species have been detected in reverse micelle systems.[45] FT-IR deconvolution also provides a semiquantitative analysis of the relative amount of water species if coupling effects are neglected, i.e., assuming the same molar extinction coefficient for each kind of OH stretching mode.

The intensity of the FT-IR absorption band of water entrapped in the lecithin reverse micelles increases by increasing the water content (see Figure S4, Supporting Information). From the integrated area, we obtained a linear dependence from w_0, with $\epsilon = 41\,000$ mol L^{-1} cm^{-1}, which is 10% higher than a previously reported value.[38]

The asymmetric OH stretching peak of water entrapped in lecithin reverse micelles cannot be fitted by two Gaussian functions; however, if three components are used (as shown in Figure 4), the calculated spectrum is in good agreement with the measured one. If the number of components is increased from three to four, the goodness of the fit, as expected, increases, but the interpretation of the results is less straightforward. In addition, although a three-component fitting procedure turned out to be quite robust and reproducible, in a four-component fitting the results seemed to be dependent on the initial guess of the parameters. Therefore, we applied the three-component fitting methodology. The three components (see Figure 4) centered at (*i*) 3300 ± 10, (*ii*) 3440 ± 10, and (*iii*) 3580 ± 10 cm^{-1} can be assigned to the OH stretching mode of (*i*) water molecules in a regular associated structure (i.e., the main component in bulk pure water), (*ii*) hydrogen-bonded dimers and other constrained structures at the interface, and (*iii*) monomeric or dimeric isolated water molecules, respectively.[38,39] In the current context, these three modes of vibration can be assigned to (*i*) bulklike-type water in the inner core of the micelles, (*ii*) interfacially bounded water molecules, and (*iii*) trapped water between the lipid hydrophobic chains.

The dependence of the deconvoluted peak areas on w_0 is presented in Figure 5. When the water content is increased, the relative abundance of bulk-type water increases from 40 to 60%, at expense of the amount of bonded water, which decreases from 55 to 30%. The area relative to the trapped water increases from about 4 to 8%. These transitions occur in the range $w_0 < 15$. No further changes are detected by increasing the water content, as the spectrum becomes similar to that of pure water.

Although with our analysis it is not possible to distinguish different types of bound water, we expect that different binding sites exist in the lecithin−water interface, and that 1-hexanol could be present at the interface. In fact, carbonyl, phosphate, and choline moieties can bind water by hydrogen bonding or ion−dipole interaction.[41−43] Previous works on this topic also suggest that water binds to the *sn*-2 carbonyl group, and not to the similar *sn*-1 carbonyl group.[41]

From the integration of the three Gaussian component peaks, we calculated the number of water molecules per molecule of surfactant present in each state, using $n_j = w_0 \times P_j$, where P_j is the fractional area ($P_j = A_j/A_{tot}$). The analysis shows that the number of trapped water molecules per molecule of surfactant seems to reach a plateau around the value of 2; however, the bulklike-type water concentration per molecule of surfactant does not reach a saturation value, instead increasing with w_0 (Table S1, Supporting Information). The concentration of interfacially bonded water also increases, from 3 to 4 molecules per molecule of surfactant in the region with $w_0 < 15$, up to 6 molecules at $w_0 = 25$ (Figure S6, Supporting Information).

Let us turn now to the samples that contain DNA. The IR spectrum of the water entrapped in reverse micelles in the presence of DNA is the average of both empty and filled micelles. Unfortunately, the instrumental sensitivity is not sufficient to distinguish the micellar solution containing DNA from those without DNA. In other words, the shape of the OH stretching band and the fitting results illustrated in Figure 5 are superimposable with those obtained for the DNA-containing reverse micelles (data not shown).

Consider that, on the basis of the calculations reported in Table 1, the cumulative internal volumes of large reverse micelles represent only a tiny amount of the total volume of the sequestered aqueous phase (less than 0.5% in both cases). Even if we granted a significant uncertainty in these figures, it is clear that the difference between the empty and DNA filled FT-IR band will be elusive.

Generally, then, we could not detect any measurable difference between the two types of micellar solutions (Table S1, Supporting Information).

Difference spectra, however, suggest a re-organization between water states, as observed at low water content. In fact, at $w_0 = 5$, the difference spectrum reveals some interesting features

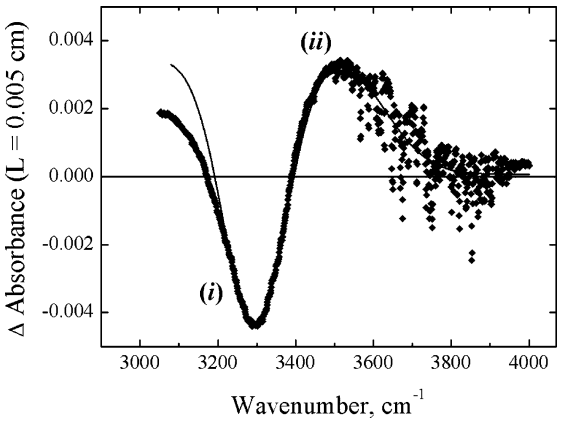

Figure 6. Difference IR spectrum (DNA-containing sample minus empty micelle sample) for the case $w_0 = 5$, plotted as points. DNA concentration in stock aqueous solution is 1 mg/mL. The negative peak corresponds to the type (*i*) stretching mode (3300 ± 10 cm^{-1}), which is related to bulklike water; the positive peak corresponds to the type (*ii*) stretching mode (3440 ± 10 cm^{-1}), which is related to bound water (fitting curves plotted as solid lines).

(Figure 6). Even if very small (less than ca. 1% of the relative area), two peaks appeared, centered at ca. 3300 and 3520 cm^{-1}, which correspond to the type (*i*) and (*ii*) OH stretching, the first being negative and the second positive.

This might suggest that in DNA-containing samples at low water content, the bound water concentration seems to be higher than in the corresponding sample without DNA. The observation agrees with the fact that DNA needs a hydration shell of water molecules. Notice that similar conclusions could also be achieved by looking at the $\tilde{\nu}_{max}$ values for the whole OH stretching band, comparing empty and DNA-containing reverse micelles (Table S1, Supporting Information). In fact, this frequency is shifted to lower wavenumbers in the case of empty reverse micelles. Unfortunately, the data available cannot be used to make a systematic analysis of the difference spectra at different w_0 values.

Discussion

It has been shown that DNA assumes a condensed form when entrapped in the water pool of lecithin reverse micelles. The term condensation has been used here in a broad sense, and the molecular details of the process are not investigated in this study. In addition, several aspects of this work necessitate a careful analysis.

The first point is relevant to the structure of the aggregate formed in the organic solvent. Although there is no doubt that reverse micelles are formed with lecithin in isooctane, it is not clear whether the particles having dimensions of about 400−700 nm are very large reverse micelles or other kinds of DNA-containing structures. An irregularly compacted DNA suspended by means of lipid molecules or a reverse vesicle architecture could be other possible structures. Although we assumed a simple spherical geometry in the calculations shown in Table 1, other morphologies (e.g., elongated or toroidal structures) could be present in the sample. With regard to the abnormal size of particles detected in this study, notice that the solubilization of entire yeast cells and other microorganisms with reverse micelles has been reported,[46] producing biologically active particles in apolar solvent, probably with a particle-size distribution in the micrometer range.

A more subtle structural question is relevant to the local w_0 value of the DNA-containing micelles. A spherical reverse micelle has a volume-to-surface ratio that increases linearly with its dimension. It is thus expected that a hypothetical large DNA-containing micelle should have a higher local value of w_0. In contrast, the constancy in size of the empty small reverse micelles in the absence and presence of DNA (around 2.5 nm) indicates, according to DLS data analysis, that the very large number of empty micelles have the macroscopically imposed w_0 value. In other words, the water segregated in the large DNA-containing particles does not affect the local water:lipid ratio in the small reverse micelles. As a corollary, the w_0 value in the large DNA-containing reverse micelles should be approximately the same as that in the small ones. The latter conclusion means that DNA occupies a significant volume of these compartments (in order to keep the w_0 value low), reaching a very high local concentration.

Another interesting aspect of our study is the remarkable stability of the DNA−water−phospholipid system. In fact, whereas in our previous work AOT-based reverse micelles exhibited physical instability,[22] time-independent CD and DLS data characterize the lecithin-based micelles described in this paper.

With the available data, only a tentative simple model for the DNA condensation in lipid compartments can be proposed. We should consider that at the very first time after the injection of a DNA solution (not-condensed DNA) in the hydrocarbon phase, a rough water-in-oil emulsion is formed, and this is quickly transformed in a reverse micelle solution by redistribution of water among empty and DNA-containing compartments (condensed DNA). The competition between DNA and lecithin headgroups for water could be the key factor of the process, which reaches, according to the results shown in this work, a sort of final equilibrium state composed of many small empty reverse micelles, whereas DNA is entrapped in relatively few larger ones. Overall, the process can be seen as a DNA dehydration process, with a consequent increase of its local concentration (Figure S7, Supporting Information). However, the molecular details of the process are still unknown.

With regard to the state of water, the present study indicates a three-state system, and presents an interesting water rearrangement dynamic that needs to be confirmed by further investigations, for example, by NMR spectroscopy. A combined FT-IR and NMR study could provide deeper insights in this characterization. However, the theoretical drawbacks already stated in the FT-IR Water Analysis section (on the small amount of water that is involved in the differential solvatation) have to be considered.

Finally, we remark here how the water content (imposed by the w_0 value) finely regulates the DNA conformation, as shown in Figure 2. On going from $w_0 = 5-7$ to $w_0 = 10$ and greater, the CD spectrum changes from a typical signal of a (+)-ψ-type spectrum to a broad negative band and then to a conventional ellipticity of B-DNA in a diluted solution.

Supporting Information Available: DLS data analysis, supplementary figures, table, and supplementary references. This material is available free of charge via the Internet at http://pubs.acs.org.

References and Notes

(1) Horn, P. J.; Peterson, C. L. *Science* **2002**, *13*, 1824−1827.
(2) Daban, J.-R. *Biochemistry* **2000**, *39* (14), 3861−3866.
(3) Matulis, D.; Rouzina, I.; Bloomfield, V. A. *J. Am. Chem. Soc.* **2002**, *124* (25), 7331−7342.
(4) Reich, Z.; Ghirlando, R.; Minsky, A. *Biochemistry* **1991**, *30* (31), 7828−7836.
(5) Bloomfield, V. A. *Curr. Opin. Struct. Biol.* **1996**, *6* (3), 334−341.
(6) Lerman, L. S. *Proc. Natl. Acad. Sci. U.S.A.* **1971**, *68*, 1886.

(7) Hanlon, S.; Brudno, S.; Wu, T. T.; Wolf, B. *Biochemistry* **1975**, *14* (8), 1648−1660.
(8) He, S. Q.; Arscott, P. G.; Bloomfield, V. A. *Biopolymers* **2000**, *53* (4), 329−341.
(9) Kankia, B. I.; Buckin, V.; Bloomfield, V. A. *Nucleic Acids Res.* **2001**, *29* (13), 2795−2801.
(10) Gueron, M.; Demaret, J. P.; Filoche, M. *Biophys. J.* **2000**, *78* (2), 1070−1083.
(11) Zuidam, N. J.; Barenholz, Y.; Minsky, A. *FEBS Lett.* **1999**, *457* (3), 419−422.
(12) Wang, Z. X.; Liu, D. J.; Dong, S. J. *Biophys. Chem.* **2000**, *87* (2−3), 179−184.
(13) Garcia-Ramirez, M.; Subirana, J. *Biopolymers* **1994**, *34* (2), 285−292.
(14) Kundu, T.; Rao, M. *Biochemistry* **1995**, *34* (15), 5143−5150.
(15) Gray, D. M.; Edmondson, S. P.; Lang, D.; Vaughan, M. *Nucleic Acids Res.* **1979**, *6* (6), 2089−2107.
(16) Arscott, P. G.; Ma, C.; Wenner, J. R.; Bloomfield, V. A. *Biopolymers* **1995**, *36* (3), 345−364.
(17) Maestre, M. F.; Reich, C. *Biochemistry* **1980**, *19* (23), 5214−5223.
(18) Livolant, F.; Leforestier, A. *Prog. Polym. Sci.* **1996**, *21* (6), 1115−1164.
(19) Shapiro, J. T.; Leng, M.; Felsenfeld, G. *Biochemistry* **1969**, *8* (8), 3219−3232.
(20) Fasman, G. D. In *Circular Dichroism and the Conformational Analysis of Biomolecules*; Plenum Press: New York, 1996; pp 433−468.
(21) Battistle, E.; Imre, E. V.; Luisi, P. L. In *Controlled Release of Drugs: Polymers and Aggregate Systems*; Rosoff, M., Ed.; VCH: New York, 1988; pp 255−276.
(22) Pietrini, A. V.; Luisi, P. L. *Biochim. Biophys. Acta* **2002**, *1562* (1−2), 57−62.
(23) Luisi, P. L., Straub, B. E., Eds. *Reverse Micelles*; Plenum Press: New York, 1982−1984.
(24) Airoldi, M.; Boicelli, C. A.; Gennaro, G.; Giomini, M.; Giuliani, A. M.; Giustizi, M. *Phys. Chem. Chem. Phys.* **2000**, *2* (20), 4636−4641.
(25) Airoldi, M.; Boicelli, C. A.; Gennaro, G.; Giomini, M.; Giuliani, A. M.; Giustizi, M.; Scibetta, L. *Phys. Chem. Chem. Phys.* **2002**, *4* (15), 3859−3864.
(26) Budker, V. G.; Slattum, P. M.; Monahan, S. D.; Wolff, J. A. *Biophys. J.* **2002**, *82* (3), 1570−1579.
(27) Becker, W. M.; Kleinsmith, L. J.; Hardin, J. In *The World of the Cell*; Addison-Wesley Longman: San Francisco, 2000; pp 488−532.
(28) Rastogi, S. C. In *Cell and Molecular Biology*; New Age International Limited: New Delhi, India, 2001; pp 228−243.
(29) Felgner, P. L.; Gadek, T. R.; Holm, M.; Roman, R.; Chan, H. W.; Wenz, M.; Northrop, J. P.; Ringold, G. M.; Danielsen, M. *Proc. Natl. Acad. Sci. U.S.A.* **1987**, *84* (21), 7413−7417.
(30) Akao, T.; Fukumoto, T.; Ihara, H.; Ito, A. *FEBS Lett.* **1996**, *391* (1−2), 215−218.
(31) Zhang, Z.; Huang, W.; Tang, J.; Wang, E.; Dong, S. *Biophys. Chem.* **2002**, *97* (1), 7−16.
(32) Peng, Q.; Luisi, P. L. *Eur. J. Biochem.* **1990**, *188* (2), 471−480.
(33) MacDonald, H.; Bedwell, B.; Gulari, E. *Langmuir* **1986**, *2* (6), 704−708.
(34) Novaki, L. P.; Pires, P. A. R.; El Seoud, O. A. *Colloid Polym. Sci.* **2000**, *278* (2), 143−149.
(35) Li, Q.; Li, T.; Wu, J. G.; Zhou, N. F. *J. Colloid Interface Sci.* **2000**, *229* (1), 298−302.
(36) Zhou, G. W.; Li, G. Z.; Chen, W. J. *Langmuir* **2002**, *18* (12), 4566−4571.
(37) McGregor, T. D.; Balcarova, Z.; Qu, Y.; Tran, M. C.; Zaludova, R.; Brabec, V.; Farrell, N. *J. Inorg. Biochem.* **1999**, *77* (1−2), 43−46.
(38) Onori, G.; Santucci, A. *J. Phys. Chem.* **1993**, *97* (20), 5430−5434.
(39) Jain, T. K.; Varshney, M.; Maitra, A. *J. Phys. Chem.* **1989**, *93* (21), 7409−7416.
(40) González-Blanco, C.; Rodríguez, L. J.; Velázquez, M. M. *Langmuir* **1997**, *13* (7), 1938−1945.
(41) Wong, P. T. T.; Mantsch, H. H. *Chem. Phys. Lipids* **1988**, *46* (3), 213−224.
(42) Cavallaro, G.; La Manna, G.; Turco Livieri, V.; Aliotta, F.; Fontanella, M. E. *J. Colloid Interface Sci.* **1995**, *176* (2), 281−285.
(43) Shumilina, E. V.; Khromova, Y. L.; Shchipunov, Y. A. *Russ. J. Phys. Chem.* **2000**, *74* (7), 1083−1092.
(44) Maitra, A.; Jain, T. K.; Shervani, Z. *Colloids Surf.* **1990**, *47*, 255−267.
(45) Hauser, H.; Haering, G.; Pande, A.; Luisi, P. L. *J. Phys. Chem.* **1989**, *93* (23), 7869−7876.
(46) Pfammatter, M.; Guadalupe, A. A.; Luisi, P. L. *Biochem. Biophys. Res. Commun.* **1989**, *161* (3), 1244−1251.